ELSEVIER

Materials Science and Engineering A 485 (2008) 46–54

MATERIALS SCIENCE & ENGINEERING A

www.elsevier.com/locate/msea

Abrasion resistance of ductile iron austempered by the two-step process

Gastón Francucci, Jorge Sikora, Ricardo Dommarco *

Grupo Tribología, Facultad de Ingeniería, Universidad Nacional de Mar del Plata, División Metalurgia, INTEMA, CONICET, Av. J.B.Justo 4302, B 7608 FDQ Mar del Plata, Argentina

Received 2 March 2007; received in revised form 18 July 2007; accepted 20 July 2007

Abstract

The present work focuses in the study of the effect that a new two-step austempering heat treatment process, developed by Putatunda, has on the mechanical properties with emphasis on the response to the abrasive wear.

A ductile cast iron melt was prepared in an industrial facility obtaining both, Y-blocks (ASTM A 897) to be used for the laboratory tests samples, and bucket tips to perform field tests by using a wheel loader.

The results show that the two-step austempering process promotes an increase in the amount of retained austenite which in turn improves most of the mechanical properties, such as ultimate stress, yield stress, hardness and impact toughness.

Two different abrasion tests were carried out in order to evaluate the material response to different tribosystems. The dry sand-rubber wheel abrasion test (ASTM G 65) was used at the lab, where the results show better wear resistance for the two-stepped ADI in comparison with conventional ADI. On the other hand, the bucket tips tested in a more severe environment, showed an opposite tendency.

Keywords: Ductile iron; Two-step austempering; Austenite content; Abrasion resistance

1. Introduction

The use of ductile iron (DI) has increased constantly since its introduction in the market in the 1950s, due to the relatively low production costs coupled with excellent mechanical properties. Subsequently, the development of austempered ductile iron (ADI) in the 1970s promoted a new and important impulse for the application of DI, thanks to its excellent combination of strength and toughness. In the later nineties the development of DI introduced the use of thin walled parts, in order to increase the strength to weight ratio and its competitiveness against light alloys.

During the nineties up today some researchers have evaluated modifications to the austempering heat treatment cycles, in order to obtain a better combination of tensile strength and toughness. For example, Nili Ahmadabadi et al. [1,2] developed the "successive-stage austempering", also called "high low austempering". The result was the reduction of the untransformed austenite volume (UAV) at the segregated regions, which in turn promoted higher impact toughness. The ultimate tensile strength was intermediate between the values obtained for a single step at $T_a = 375$ and 315 °C, but the elongation was better than in both cases. More recently, Nili Ahmadabadi et al. [3] studied the effect of the successive austempering on the tribological behavior of ductile iron by using a pin-on-ring test rig.

Bayati et al. [4] used a "stepped austempering" to overcome the decrease in the mechanical properties promoted by the UAV observed in alloyed ADI at the last to freeze (LTF) segregated regions. By using the second step, the authors were able to complete the bainitic reaction and to obtain a significant improvement in the relation between ultimate tensile strength, elongation and impact toughness.

Based on the results of Nili Ahmadabadi et al. and Bayati et al., Hsu and Chuang [5] studied the influence of a "stepped austempering" (also called two-step by the authors), on the fracture toughness of ADI, comparing the results with conventional austempering at the same temperatures. They found a matrix with a more interwoven ausferrite and a higher amount of retained austenite with respect to the conventional austempering. At the same time the hardness was typical of a low austempering temperature, but the fracture toughness resulted typical of higher austempering temperature ADI.

Also Hafiz [6,7] has experimented with a "variable austempering" process by following two different routes (increasing

* Corresponding author.
E-mail address: dommarco@fi.mdp.edu.ar (R. Dommarco).

0921-5093/$ – see front matter © 2007 Elsevier B.V. All rights reserved.
doi:10.1016/j.msea.2007.07.081

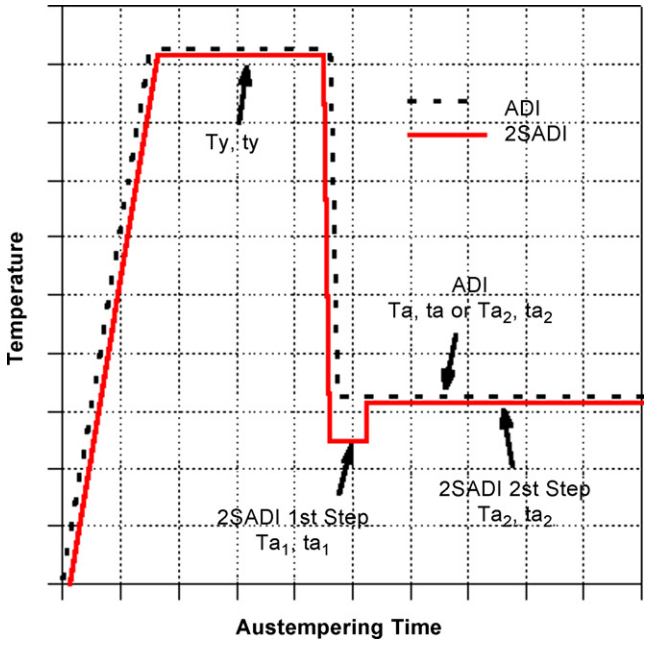

Fig. 1. ADI and 2SADI heat treatment cycles.

and decreasing T_a) and comparing to standard austempering cycles. The mixed microstructures obtained by the variable austempering appears to have higher elongation and impact toughness than the isothermally austempered ones.

It was considered by Putatunda [8], that the yield strength of ADI depends on the fineness of the ferrite needles, and that the fracture toughness depends on the $X_\gamma C_\gamma$ parameter, where X_γ is the austenite volume fraction and Cγ is the austenite carbon content. Then, a new austempering heat treatment cycle was proposed, involving a first step with a high undercooling, in order to increase the nucleation rate of ferrite, followed by a second step at higher temperature, with the aim of increase the diffusion rate and also the carbon content in austenite. So, an ADI with a combination of high strength and high fracture toughness may be obtained. The results confirmed that the "two-step austempered" ADI (2SADI) could improve both, the fracture toughness and at the same time the tensile strength.

In a later publication, Yang and Putatunda [9] developed a modification to the two-step austempering (Fig. 1). The first step, with a high undercooling by quenching at $T_a = 260\,^\circ$C for $t_a = 5$ min, and after that the temperature was raised for the second step up to a desired level in the range of $T_a = 290$–$400\,^\circ$C for $t_a = 2$ h, by changing to a second salt bath. The two-step ADI (2SADI) showed higher $X\gamma$ and $C\gamma$, exhibiting higher strength and hardness and lower elongation, than that obtained with the single step austempering. The 2SADI also yields to a lower strain hardening exponent [10] and a higher near threshold fatigue crack growth rate [11].

1.1. Abrasion resistance of ADI

The microstructure of ADI usually has very good abrasion resistance [12,13]. It is able to respond well to the low stress abrasion, when using low austempering temperatures (high hardness), and also to resist high stress abrasion when using high austempering temperatures (low hardness, high ductility) [14]. In fact, the presence of the very ductile microconstituents, ferrite and austenite, has a strong influence in the ability of ADI to consume energy during abrasion, plus the energy consumption associated to austenite transformation into martensite due to the stress assisted or strain induced mechanisms [14,15].

Yang and Putatunda [16] also studied the effect of the two-step austempering on the abrasion resistance of ADI by using a pin on disk test rig with a 150 mesh garnet abrasive, showing lower weight loss than the single step ADI variant. The authors found that the weight loss decreased by ∼1% at austempering temperatures between $T_a = 340$–$380\,^\circ$C up to ∼5% at $T_a = 280\,^\circ$C.

Using the high–low stepped austempering process Nili Ahmadabadi et al. [3] also studied the tribological behavior of ADI, in this case by using a pin-on-disk test rig. The results showed that delamination took place and that the influence on the microstructure, i.e. higher retained austenite and carbon in austenite, promoted a ∼15% increase in the wear resistance with respect to the conventional high temperature austempering but a ∼15% decrease with respect to the low austempering temperature.

It was thought that the higher retained austenite content promoted by the 2SADI, could also promote an improvement in the abrasion resistance. In order to evaluate this possibility, the 2SADI process proposed by Putatunda was chosen for the present study, since austenite volume fraction may increase between 10 and 30% depending on the austempering temperature [9]. Therefore, the present work focuses on the study of the influence that the two-step austempering process has on the abrasion resistance of ADI under two different environments. One of them was the low stress condition imposed in the lab by the "dry sand-rubber wheel abrasion test" (ASTM G 65) and the other was the high stress conditions imposed in field tests to wheel loader bucket tips.

2. Experimental procedure

2.1. Sample preparation and microstructural analysis

An industrial ductile iron heat was prepared in a 1500 kg capacity 50 Hz induction furnace employing regular quality raw materials. Inoculation and nodulization procedures were carried out in a 500 kg ladle with nodulization pocket by using conventional techniques. Y-blocks according to the ASTM A 395 standard and bucket tips were cast into sand molds from a single heat. The final chemical composition of the heat was determined by means of a Baird Spark Emission Optic Spectrograph with a DV6 excitation source.

The samples for laboratory tests were machined from the Y-blocks. After rough machining both, the laboratory samples and the tips were heat treated by single and two-step austempering cycles, Fig. 1, using the parameters listed in Table 1. The austenitizing stage was carried out in an electric furnace, while the austempering steps were performed in two

Table 1
Sample identification and heat treatment parameters

Identification	Heat treatment type	Austenit. temperature, T_γ (°C)	Austempering parameters, temperature (°C)/time (min)	
			First step T_{a1}/t_{a1}	Second step T_{a2}/t_{a2}
ADI 260	One step			260/120
ADI 280	One step			280/120
ADI 320	One step			320/120
ADI 360	One step	920		360/120
2SADI 280	Two step		260/6	280/120
2SADI 320	Two step		260/6	320/120
2SADI 360	Two step		260/6	360/120

salt baths having 150 and 60 l capacity, for the first and second austempering steps, respectively.

The metallographic sample preparation was carried out by using standard techniques. Metallographic etching was performed employing 2% nital. The nodularity and nodule count values were measured by using both, the ASTM A 247 standard and the Image Pro Plus software. Worn surfaces were studied by using optical and scanning electron microscopes.

In order to determine the retained austenite content in the ausferrite, X-ray measurements were carried out by using a Phillips goniometer with the X-ray tube operating at 40 kV/30 mA. Co Kα radiation was used scanning from 48° to 54° of 2θ with a data collecting velocity of 1°/min. The retained austenite was measured on surfaces obtained by classical metallographic preparation and then etched up to a depth of ~40 μm, by using NHO_3 20% in order to eliminate the deformed layers.

2.2. Mechanical characterization

The hardness was measured by using the Brinell method with a 2.5 mm tungsten carbide ball and 187.5 kg load ($HBW_{2.5/187.5}$), and the reported values are the average of a least four determinations. The tensile tests were performed according to the ASTM E 8 standard, at a constant strain rate lower than 4×10^{-4} mm/seg, and the reported values for tensile strength, yield strength and elongation are the average of three determinations. The impact toughness tests were carried out according to the ASTM E 23 standard and the reported values in this case are the average of four tests on unnotched specimens.

2.3. Wear resistance tests

The abrasive wear resistance of the samples was evaluated in the lab by means of the "Dry Sand/Rubber Wheel Test", according to ASTM G 65 standard, using procedure A. The relative wear resistance index, E, was obtained by the ratio between the volume loss experienced by a reference material (ΔV_R), (in this case a SAE 1010 steel) and by the ductile iron sample (ΔV_S), according to Eq. (1). Weight loss values were measured by means of a 0.1 mg precision scale and then converted into volume loss by using the density value measured for this iron heat.

$$E = \frac{\Delta V_R}{\Delta V_S} \quad (1)$$

Table 2
Chemical composition [wt%]

C	Si	Mn	P	S	Mg	Cr	Ni	Mo	Cu
3.5	3.0	0.4	0.03	0.03	0.02	0.08	0.3	0.17	1.0

Balance, Fe.

The relative wear resistance of the experimental wheel loader bucket tips was evaluated as a function of the hours in service in a 2 m^3 bucket on a 110 hp wheel loader. Of the eight tip positions on the bucket, the two located at the center were used to evaluate the performance of the sample tip and the reference material tip in this case made of a conventional ADI austempered at $T_a = 280$ °C. The tips were removed periodically during service, weighted and then replaced in the same position in the bucket. The weight losses of the reference ADI tip (ΔP_R) and the 2SADI tips (ΔP_S), Eq. (1), were measured by means of an electronic scale with 5 g sensitivity, and then converted into volume losses ΔV_R and ΔV_S, respectively.

3. Results and discussion

3.1. As cast material characterization

Table 2 lists the chemical composition of the heat used in the present paper. The equivalent carbon was slightly hypereutectic (EC = 4.5), giving the microstructure shown in Fig. 2. In

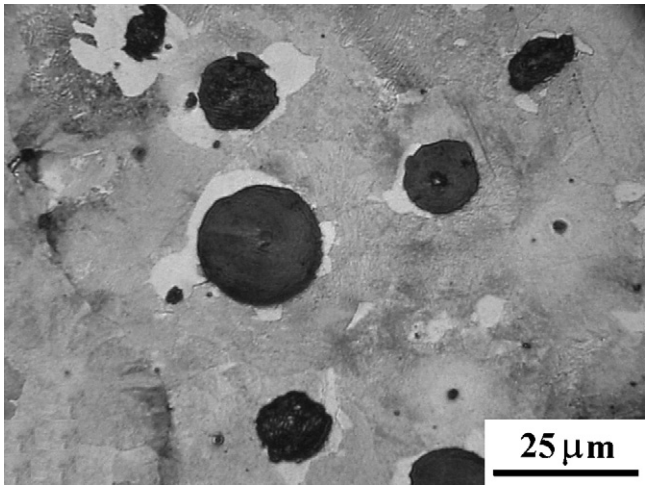

Fig. 2. As cast microstructure showing details of the matrix and bull's eye ferrite.

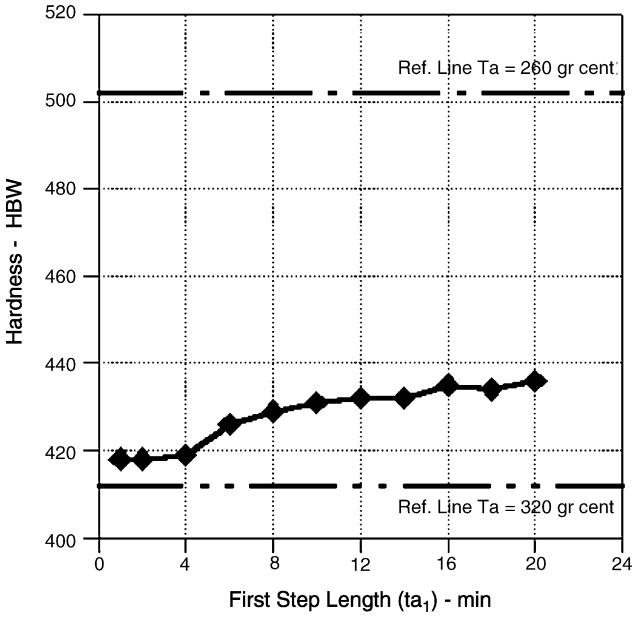

Fig. 3. Final hardness as a function of the first step length (t_{a1}).

the as cast condition, the matrix was predominantly pearlitic, containing small amounts of bull's eye ferrite.

3.2. Determination of the first step length (t_{a1})

The first step length (t_{a1}) is very important for the stepped heat treatment, in order to obtain the desired microstructure. Then, t_{a1} must be long enough to promote an intense ferrite nucleation, but at the same time not too long in order to make those nuclei to grow at the second step austempering temperature (T_{a2}) along the specified second step austempering time (t_{a2}).

The material sensibility to the first step length was studied by monitoring the final hardness as a function of t_{a1}, Fig. 3, using fixed first step and second step temperatures, $T_{a1} = 260\,^{\circ}C$ and $T_{a2} = 320\,^{\circ}C$, respectively, and $t_{a2} = 120$ min. It was found that as t_{a1} increases the hardness was almost constant during the first 4 min and then begun to increase starting at about $t_{a1} = 6$ min. Microstructural changes were also observed, as it will be discussed later. Taking this information into account besides the values used by Putatunda et al. [8–12] the authors chose $t_{a1} = 6$ min for all the two-step heat treatments.

3.3. Microstructural characterization

Fig. 4 shows the microstructures corresponding to the ADI and 2SADI samples, respectively. The microstructures were the typical expected for austempering, with an acicular ferrite morphology for the low heat treatment temperature, $T_a = 280\,^{\circ}C$ (Fig. 4a), and a feathery ferrite morphology for the high temperature, $T_a = 360\,^{\circ}C$ (Fig. 4c). It is also visible the presence of white regions were the transformation has not proceed (absence of ferrite needles or feathers), corresponding to the UAV volume. These regions are in concordance with the LTF zones due to the effect produced by the presence of micro-segregation of the alloying elements, such as Mn and Mo, which make the austenite more stable at room temperature.

The 2SADI microstructures (Fig. 4d–f) resulted very similar to that of the ADI, when comparing the aspect of the ferrite needles and/or feathers as a function of the austempering temperature. Nevertheless, as a result of the stepped heat treatment, the 2SADI microstructures appears to have less and smaller UAV regions.

3.4. Retained austenite content

The X-ray diffraction diagrams were obtained for $48^{\circ} < 2\theta < 54^{\circ}$, where the austenite ($\gamma$-1 1 1) and ferrite ($\alpha$-1 1 0) peaks are located when the Co Kα radiation is used. The results show that the retained austenite (γ_{ret}) increases as the austempering temperature also increases. It is considered that at the low austempering temperatures the ferrite needles grow rapidly within the austenite due to the high driving force, but at the same time the carbon diffusion is low and austenite saturates in carbon, precipitating ε carbides. The reaction proceeds continuously and the resulting amount of γ_{ret} is low [17]. On the other side, when the austempering temperature is high the driving force is lower, but the carbon diffusion is higher. Thus, during the growing process of ferrite, carbon migrates to the surrounding austenite enriching this phase up to ~2% C and then ferrite growing is arrested [17]. With this carbon content in the austenite the M_s temperature decreases and therefore higher amount of γ_{ret} is obtained.

The quantitative data obtained from these diagrams are listed in Table 3. The results also show that there is an increase of γ_{ret} in 2SADI with respect to ADI at the three austempering temperatures evaluated (Fig. 5). This is attributed to the presence of finer ferrite needles which in turn delay the carbon saturation. It is important to point out that these results may not be concluding because the observed differences are within the error of the equipment used, nevertheless the trend was consistent for all the austempering temperatures and it is also in agreement with measurements made by other researchers [8,9].

3.5. Mechanical properties

The results of the tensile tests are listed in Table 4, with the reported values obtained as the average of four samples. There is almost no difference between ADI and 2SADI samples when comparing the yield stress and also there are small differences when the ultimate stress is considered (Fig. 6). Nevertheless, even though the observed differences may be within

Table 3
Retained austenite content for ADI and 2SADI samples

Austempering temperature (°C) T_a or T_{a2}	Retained austenite (%)		
	ADI	2SADI	% Increase
260	23.0	–	–
280	22.6	23.8	5.3
320	27.5	28.9	5.1
360	39.0	40.7	4.3

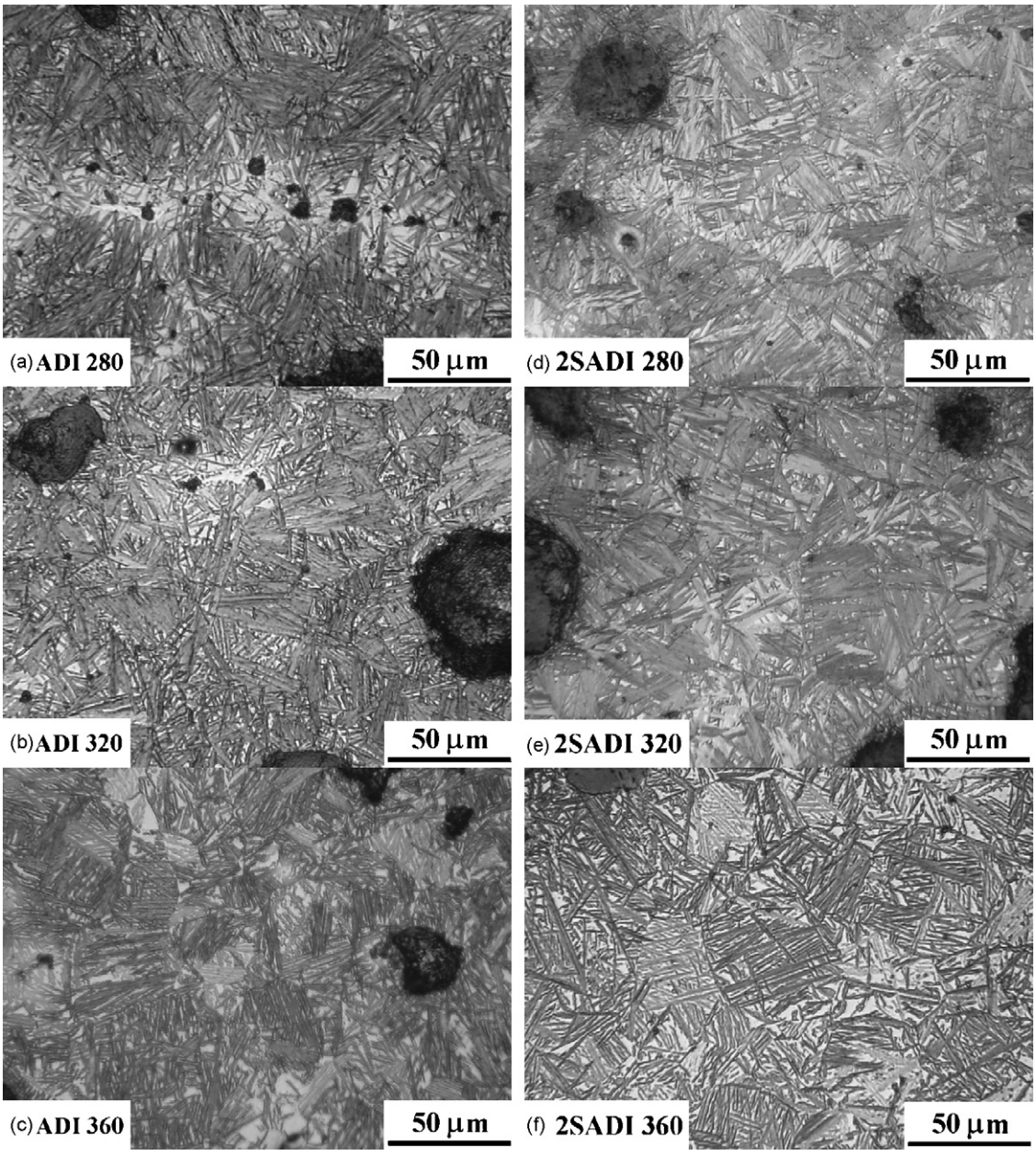

Fig. 4. Microstructure of ADI samples, (a) ADI 280, (b) ADI 320, (c) ADI 360, and 2SADI samples (d) 2SADI 280, (e) 2SADI 320, (f) 2SADI 360.

the errors of the methodologies used, it can be remarked that in all cases the strength values (yield or ultimate) were higher for the 2SADI and also the high ultimate strength value obtained for the 2SADI 280 samples. With regards to the elongation of the 2SADI variants, the response was in accordance with what it could be expected from the higher stress values, i.e. lower elongation values for the 2SADI variants with respect to ADI.

The impact toughness values reported in Fig. 7 and Table 5 were obtained as the average of four unnotched samples,

Table 4
Tension tests results with σ_{n-1} values in brackets

Austempering temperature (°C)	Yield strength $\sigma_{0.2}$ (MPa)		Ultimate tensile strength σ_{UTS} (MPa)		Elongation (%)	
	ADI	2SADI	ADI	2SADI	ADI	2SADI
260	1185 (75)	–	1431 (4.9)	–	2.5 (0)	–
280	1102 (90)	1139 (55)	1408 (32)	1512 (45)	4.0 (0.9)	3.4 (0.3)
320	982 (23)	989 (70)	1255 (49)	1296 (65)	4.6 (0.5)	4.8 (0.7)
360	715 (50)	717 (55)	1035 (70)	1058 (22)	6.9 (1.2)	5.1 (1.2)

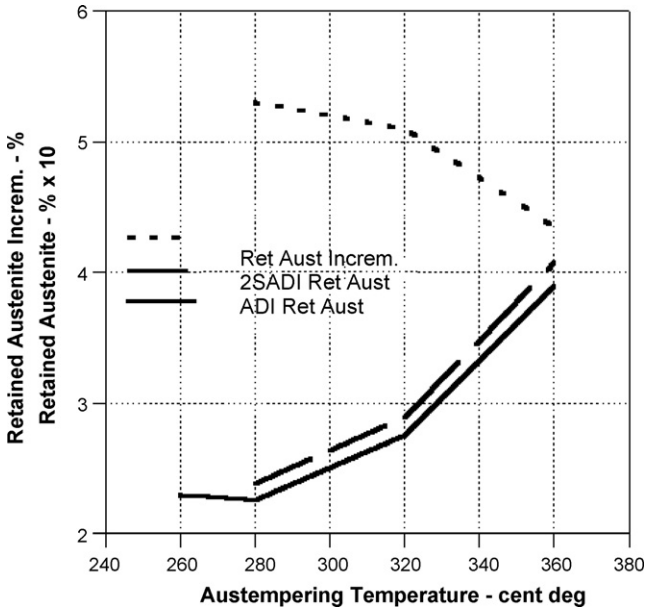

Fig. 5. Retained austenite content (γ_{ret}) values for the different ADI and 2SADI variants.

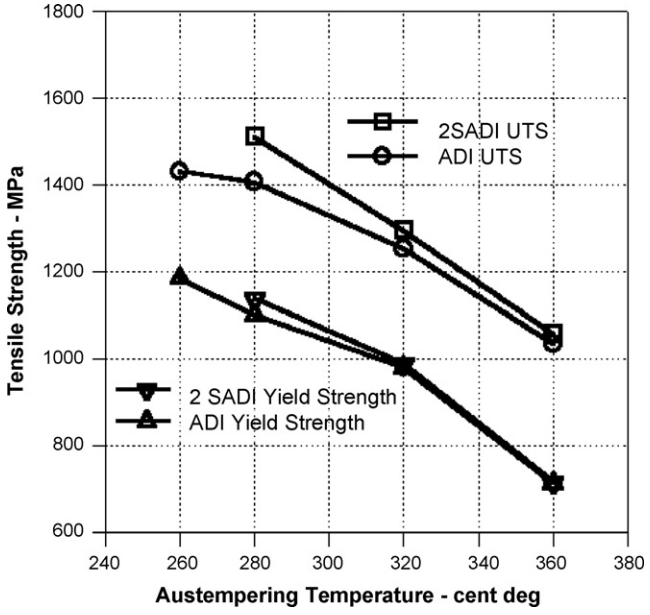

Fig. 6. Proof stress and tensile strength of ADI and 2SADI as a function of T_{a1} and T_{a2}.

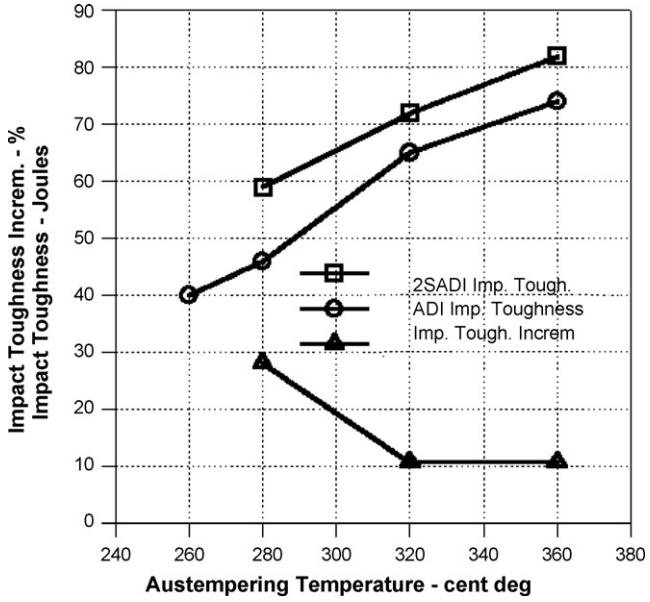

Fig. 7. Impact toughness of ADI and 2SADI as a function of T_{a1} and T_{a2}.

showing the typical response observed for ADI, increasing as the austempering temperature increase. The same trend with respect to T_{a2} was observed for the 2SADI variants, but surprisingly these values were higher than those obtained for ADI. This result would not be expected when taking into account the tensile properties (strength and elongation) and also the increase in hardness shown in Fig. 8, since the typical response for irons and steels show a reduction in impact toughness when strength and hardness increase.

3.6. ASTM G 65 assessment

Using the volume loss values obtained from the wear tests the relative wear resistance index "*E*" was calculated as the relation between the volume losses of the reference material with respect to the ductile iron sample, i.e. the higher the *E* value the higher the wear resistance. In order to calculate the *E* values reported in Table 6, the density of the ductile iron was measured giving a value of $\delta \approx 7.1$ g/cm^3.

The abrasion resistance increases as the austempering temperature decreases, i.e. with an increase in hardness, either for the ADI or the 2SADI variants (Fig. 9). Similar to the other properties evaluated, the *E* values of the 2SADI were higher than that of ADI, again with the higher % increase (in this case ∼29%)

Table 5
Impact toughness and hardness of ADI and 2SADI variants

Austempering temperature (°C)	Impact toughness (J)		Hardness ($HBW_{2.5/187.5}$)	
	ADI	2SADI	ADI	2SADI
260	40 (2.0)	–	498 (9.1)	–
280	46 (3.9)	59 (8.3)	456 (6.3)	481 (4.6)
320	65 (5.0)	72 (8.9)	420 (4.5)	433 (3.5)
360	74 (4.3)	82 (5.7)	356 (2.3)	361 (4.5)

σ_{n-1} values in brackets.

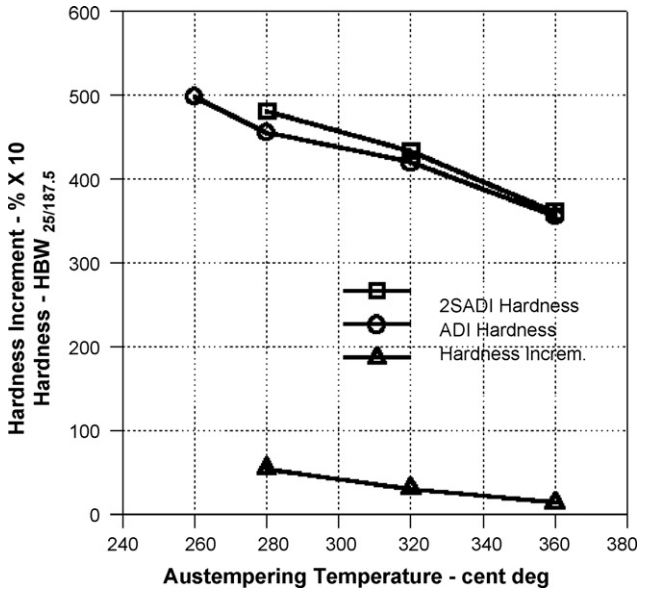

Fig. 8. Hardness of ADI and 2SADI as a function of T_{a1} and T_{a2}.

Table 6
Laboratory tests (ASTM G 65) relative wear resistance (E)

Austempering temperature (°C)	Relative wear resistance, E	
	ADI	2SADI
260	2.46 (0.06)	–
280	1.61 (0.14)	2.08 (0.11)
320	1.42 (0.02)	1.44 (0.04)
360	1.22 (0.05)	1.36 (0.16)

σ_{n-1} values in brackets.

for the variant austempered at $T_{a2} = 280\,^{\circ}C$. This increment was much higher than that reported by other authors even though it must be taken into account that different tribosystems were used.

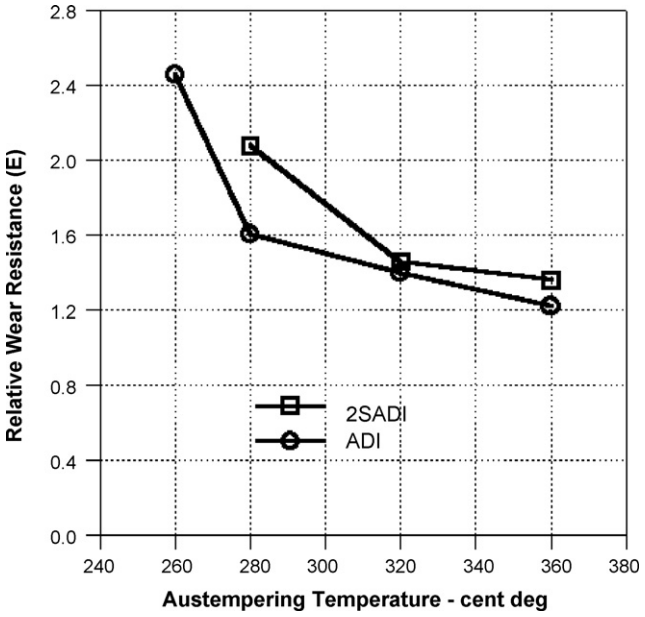

Fig. 9. Relative wear resistance (E) versus austempering temperature. Laboratory tests, ASTM G 65, ref. mat. SAE 1010.

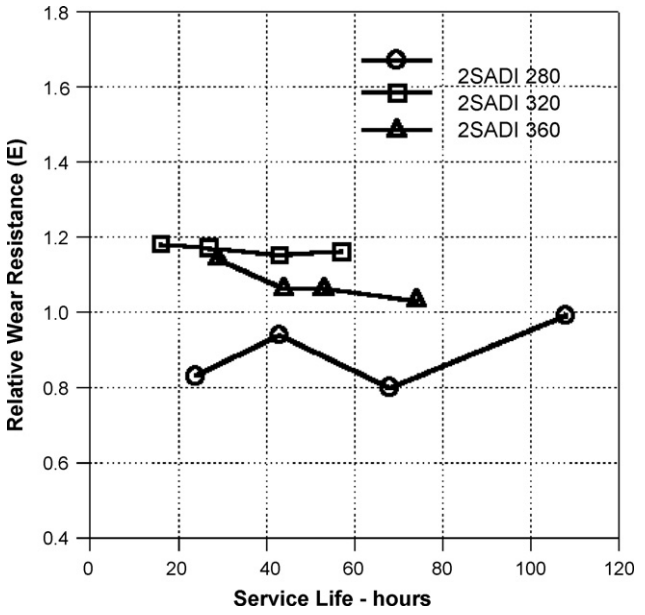

Fig. 10. Relative wear resistance (E) versus service life. Field tests on bucket tips, ref. mat. ADI 280.

3.7. Tips service assessment

When the ADI and 2SADI bucket tip samples were evaluated in the field, i.e. under different and more severe abrasive conditions than that imposed in the lab, the response was opposite. This means that the wear resistance of the tips tends to increase when T_a increases. Fig. 10 presents these results in terms of E versus service life, in this case using ADI 280 as a reference material, showing that the material behaves different with respect to the hardness. This is also shown in Fig. 11, in this case as E versus hardness, where the abrasion resistance

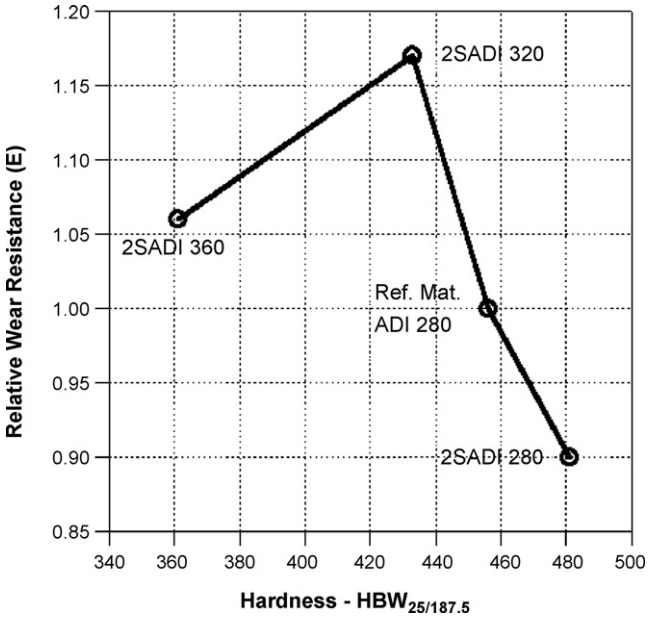

Fig. 11. Relative wear resistance (E) versus hardness. Field tests on bucket tips, ref. mat. ADI 280.

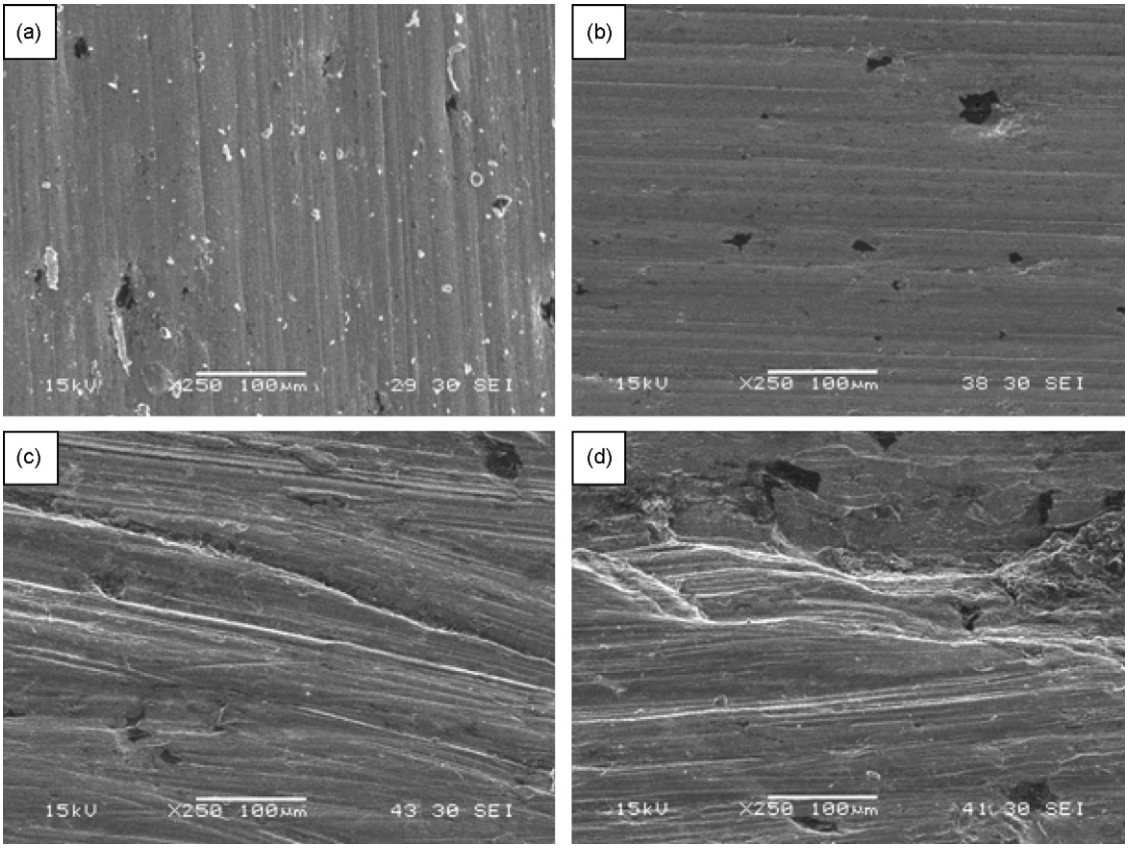

Fig. 12. Wear scars (a) ADI 280, laboratory test ASTM G 65, (b) 2SADI 360, laboratory test ASTM G 65, (c) ADI 280 bucket tip test, (d) 2SADI 360 bucket tip test. Samples tilted 30° perpendicular to the longitudinal axis.

decreases as hardness increases, particularly for the range 420–480 $HBW_{2.5/187.5}$.

The different abrasive conditions between laboratory and field tests produce differences in the wear scars. Fig. 12a and b show the surface of the test samples for ADI 280 and 2SADI 360 tested in the lab, respectively. The wear scars of the same material variants tested in the field, Fig. 12c and d, show that the material was able to accommodate more plastic deformation. Even though hardness decreases and the furrows sections increase, the abraded material deforms instead of being removed as a chip and therefore more abrasive passes or energy consumption are needed to produce the abrasive wear.

For the case of the samples 2SADI 360, Fig. 11, the decrease in hardness was not compensated by the increase in ductility leading to a lower wear resistance ($E \sim 1.06$). Similar results were previously reported for ADI bucket tip samples austempered in the range 240–360 °C [14,18] where the abrasion resistance increased continuously from $T_a = 240$ °C up to $T_a = 320$ °C, and begins to decrease at about $T_a \approx 340$ °C.

The previous hypothesis regarding the increase in abrasion resistance due to a higher retained austenite content promoted by the two-step austempering process could not be confirmed due to the small increase obtained in γ_{ret}. Nevertheless, the higher hardness of the 2SADI affected the abrasion resistance showing

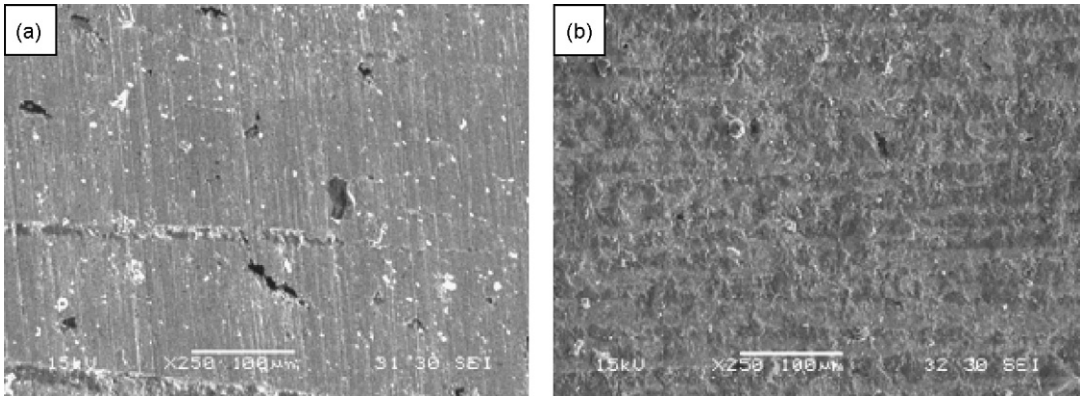

Fig. 13. ASTM G 65 wear scar, (a) inlet zone, (b) middle zone. Samples tilted 30° perpendicular to the longitudinal axis.

an increment for the laboratory test conditions but a decrease under the field test conditions. In this respect, these results have shown the same trends as those previously reported [14,18].

The modification to the conventional austempering heat treatment cycle to a stepped austempering by introducing the low temperature first step has produced the more noticeable microstructural changes and mechanical improvements for the 2SADI 280 variant. This result was unexpected since this heat treatment cycle was very similar to that used for ADI 280, with the only difference given by the use of the first step at $T_{a1} = 260\,^{\circ}C$ and $t_{a1} = 6$ min. On the other hand, the 2SADI 360 having the greater difference with respect to the ADI 360 cycle has shown little effect on microstructure and then on mechanical properties. This topic needs further investigation.

Besides the comparison of the wear scars of the different tribosystems used in the present work, it was also studied in particular different zones of the ASTM G 65 wear scar, a wear test classified by this standard as three body abrasion. Probably, this classification was originated in the application of systems analysis to tribology [19]. Nevertheless, most of this scar surface has the characteristic aspect corresponding to two body abrasion considering its manifestation [19], i.e. parallel and long furrows with almost constant width, as shown in Fig. 13a. Only a minor part of the wear scar corresponding to the inlet zone shows the aspect corresponding to the body abrasion, i.e. short furrows with continuously changing direction and width as shown in Fig. 13b.

4. Conclusions

The use of the two-step austempering process produce microstructural changes with respect to conventional one step austempering, particularly a further advance of the ausferrite transformation in the micro-segregated regions corresponding to the last to freeze zones.

The microstructural changes were reflected as improvements in most of the mechanical properties, such as ultimate stress, yield stress and hardness, and a decrease in elongation. Based on these results it is usually expected a decrease in impact toughness, nevertheless, this property increased for all the austempering temperatures evaluated.

The main purpose of this paper was to evaluate the effect of the stepped austempering heat treatment on samples tested under abrasive conditions. It was found that the results depend on the tribosystem severity. Therefore, under the low stress abrasive conditions imposed by the ASTM G 65 abrasion test, the 2SADI showed higher wear resistance than ADI, and the performance increased with material hardness. On the other hand, under the high stress abrasive conditions imposed to the bucket tips in the field tests, the performance tends to increase as hardness diminishes and ductility increases.

The more noticeable microstructural changes and mechanical improvements were obtained for the 2SADI 280 variant. This appear to be unexpected since this heat treatment cycle does not involve an important difference between the austempering temperature of the first step ($T_{a1} = 260\,^{\circ}C$) and the second step ($T_{a1} = 280\,^{\circ}C$) in comparison with the 2SADI 360 ($T_{a1} = 360\,^{\circ}C$).

References

[1] M. Nili Ahmadabadi, T. Ohide, E. Niyama, Effects of succesive-stage austempering on the structure and impact strength of high-Mn ductile iron, Cast Met. 5 (2) (1992) 62–72.
[2] M. Nili Ahmadabadi, E. Niyama, T. Ohide, AFS Trans. 102 (1994) 269–278.
[3] M. Nili Ahmadabadi, H.M. Ghasemi, M. Osia, Wear 231 (1999) 293–300.
[4] H. Bayati, R. Elliot, G.W. Lorimer, Mater. Sci. Technol. 11 (1995) 1007–1013.
[5] C.-H. Hsu, T.-L. Chuang, Metall. Mater. Trans. A 32 (2001) 2509–2513.
[6] M. Hafiz, Mater. Sci. Eng. A 340 (2003) 1–7.
[7] M. Hafiz, AFS Trans. 111 (2003) 03–035.
[8] S.K. Putatunda, Mater. Sci. Eng. A 315 (2001) 70–80.
[9] J. Yang, S.K. Putatunda, Mater. Des. 25 (2004) 219–230.
[10] J. Yang, S.K. Putatunda, Mater. Sci. Eng. A 382 (2004) 265–279.
[11] J. Yang, S.K. Putatunda, Mater. Sci. Eng. A 393 (2005) 254–268.
[12] Ductile Iron Data for Design Engineers, QIT-Fer et Titane Inc., 1990, pp. 1–33 (Chapter IV).
[13] W.S. Zhou, D.Q. Zhou, S.K. Meng, Cast Met. 6 (2) (1993) 69–75.
[14] R. Dommarco, I. Galarreta, H. Ortíz, P. David, G. Maglieri, Wear 249 (2001) 100–107.
[15] S. Shepperson, C. Allen, Wear 121 (1988) 271–287.
[16] J. Yang, S.K. Putatunda, Mater. Sci. Eng. A 406 (2005) 217–228.
[17] R. Elliot, Cast Iron Technology, Pub. Butterworth & Co., 1988, pp. 126–164 (Chapter 4).
[18] S. Laino, H. Ortíz, R. Dommarco, Relación Capacidad de Deformación-Resistencia a la Abrasión de Uñas para Pala Mecánica Fabricadas en ADI, Jornadas SAM CONAMET 2005, 18-21 de octubre, Mar del Plata, Argentina, ISBN 987-22443-0-8.
[19] J. Gates, Wear 214 (1998) 139–146.